Journal of Visualization, Vol. 11, No. 2 (2008)173-180

Regular Paper

Visualization of Turbulence Structure in Unsteady Non-Penetrative Thermal Convection Using Liquid Crystal Thermometry and Stereo Velocimetry

Fujisawa, N.*, Watanabe, M.* and Hashizume, Y.*

* Visualization Research Center, Niigata University, 8050 Ikarashi-2, Niigata, 950-2181, Japan.
E-mail: fujisawa@eng.niigata-u.ac.jp

Received 31 October 2007
Revised 29 December 2007

Abstract : Temperature and velocity fields in unsteady non-penetrative turbulent thermal convection of a horizontal fluid layer are measured in horizontal and vertical planes simultaneously using the combined liquid-crystal thermometry and stereo particle image velocimetry (PIV) with high spatial and temporal resolution. The result shows the formation of convection pattern across the fluid layer, which originates from the spoke structure over the heated surface. The upward fluid motion is generated from the intersection of the bursting lines of the spoke structure, while the downward motion is induced by the low temperature fluid directing toward the center of the spoke structure. Thus, the large-scale convective motion is produced in the fluid layer through the motion of spoke structure. The POD analysis of the temperature and velocity eigenfunctions shows the existence of large-scale motion in the fluid layer, which supports the observed convection pattern near the heated boundary and in the middle of the fluid layer.

Keywords : Visualization, Turbulence, Thermal convection, Liquid crystal, Thermometry, Velocimetry.

1. Introduction

The thermal convection of a horizontal fluid layer is a fundamental flow configuration for studying the behavior of thermal turbulence. When the horizontal fluid layer is heated from below with a constant heat flux and is insulated at the above boundary, such convection pattern is called unsteady non-penetrative thermal convection. This convection pattern shares the common features to the lower half of the fluid layer under the penetrative thermal convection of atmospheric boundary layers. Therefore, the unsteady non-penetrative thermal convection has been considered as a fundamental flow configuration for studying the general characteristics of thermal convection.

Since the pioneering visualization research by Sparrow et al. (1970), the structure of thermal turbulence has been a topic of interests for many years, and was studied experimentally (Willis and Deardorff, 1979; Tamai and Asaeda, 1984; Castaing et al., 1989; Gluckman et al., 1993; Prasad and Gonuguntla, 1996; Fujisawa and Adrian, 1999) and numerically (Schmidt and Schumann, 1989; Balachandar, 1992). For details of the classical studies see the review paper by Adrian et al. (1986). These studies show that the polygonal spoke structure is generated near the heated boundary and the large-scale fluid motion is generated in the middle of the fluid layer. Although the spoke structure contributes to the heat-transfer characteristics in the thermal convection, the mechanism is not fully understood in spite of its importance. It is known that the size of the spoke structure and

the periodic generation of thermals are functions of flux Rayleigh number (Sparrow et al., 1970). However, the detailed quantitative description of the thermal turbulence especially at high Rayleigh number, in the sense of application, has not been fully understood in literature due to the lack of experimental technique for characterizing the unsteady three-dimensional thermal flows (Fujisawa and Adrian, 1999).

In recent years, the thermal turbulence has been studied using visualization techniques (Dabiri and Gharib, 1996; Funatani and Fujisawa, 2002; Banerjee et al., 2006; Inagaki et al., 2006). The three-dimensional temperature and velocity field in Rayleigh-Bernard convection is measured using scanning liquid-crystal thermometry and a stereo velocimetry (Fujisawa et al., 2005). Although such measurement provides new insight into the quantitative nature of thermal turbulence in the Rayleigh-Bernard convection, the spoke structure near the heated boundary has not been fully understood due to the low spatial resolution of measurement in the scanning direction of light sheet. In order to clarify the relationship between the spoke structure and thermals, it is necessary to measure simultaneously the temperature and velocity field near the heated boundary with high resolution in space and time. Such observation can be realized by the simultaneous measurement of temperature and velocity field in multiple planar sections using the combined liquid crystal thermometry and stereo velocimetry, but has not been studied in literature.

The purpose of this paper is to study the visualization and measurement of turbulence structure of unsteady non-penetrative thermal convection by simultaneously measuring the temperature and velocity field in the horizontal and vertical planes using the combined liquid-crystal thermometry and stereo velocimetry, and by analyzing the data with the aid of snapshot POD method.

2. Experimental Apparatus and Procedures

2.1 Experimental Setup

The experimental test section for unsteady non-penetrative thermal convection is shown in Fig. 1, which consists of the test vessel having square horizontal dimensions of 400 mm × 400 mm and 60 mm in height. A working fluid of water is heated from below using an electrical heater mat, while it is insulated at the top boundary. The bottom boundary was made of copper material, and the top and side boundaries are made of transparent acrylic-resin material for heat insulation and flow visualization purposes. In order to minimize the heat loss from the side boundaries, the heat insulation material was covered over the side boundaries except for the windows for observation and illumination. Note that this test vessel is also used for the temperature calibration of liquid crystals by making a uniform temperature field with the use of underwater pump.

2.2 Imaging Technique

The simultaneous measurement of temperature and velocity field at two orthogonal planar sections of thermal convection is carried out using the combined liquid-crystal thermometry and stereo velocimetry, which is shown in Fig. 1. This system consists of two color 3CCD cameras for stereo observation of the horizontal planar section from the above and a color 3CCD camera for the

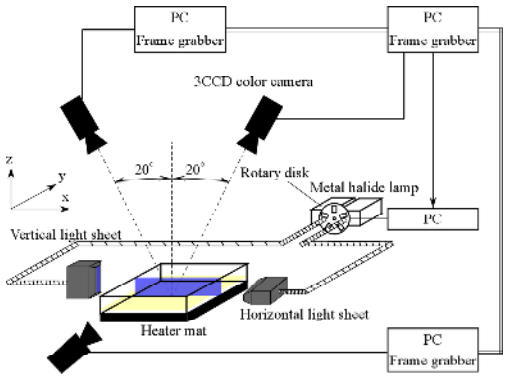

Fig. 1. Experimental setup.

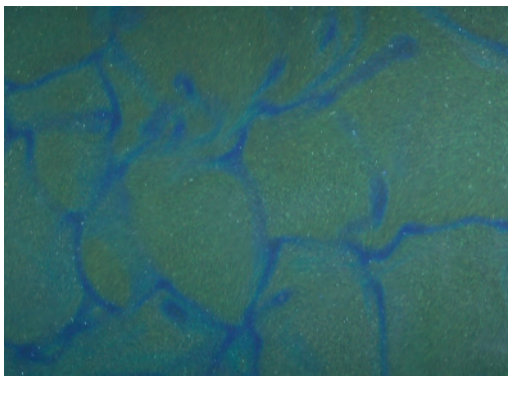

Fig. 2. Visualization of spoke structure over a heated boundary (70 mm x 100 mm).

observation of vertical plane from the side. Note that these cameras are operated synchronously. Therefore, three components of velocity and temperature are measured in the horizontal plane near the heated boundary (y = 5 mm) and two components of velocity and temperature are measured in the vertical plane at the center of the test section. The target area of interest is 80 mm × 50 mm in the horizontal plane and is 80 mm × 60 mm in the vertical plane. Note that the spatial resolution of the color 3CCD cameras is 768 × 494 pixels for each component of RGB with 8 bit. These output signals are digitized into 640 × 480 pixels by the frame grabber installed to personal computers. In the stereo observation of the horizontal plane, the off-axis half-angle of the stereo camera was set to 20 deg.

The illumination was provided from a light sheet from metal halide lamp of power 250 W. The light sheet was chopped by a rotary disk and directed to the horizontal and vertical planes of the test section via the optic fibers and the cylindrical lens. Note that the rotary disk is controlled by the vertical blanking signal from the camera to provide an alternative illumination of horizontal and vertical light sheet of 5 mm in thickness. The imaging rate is 7.5 Hz for each plane of measurement. Although there exits a short time lag of 1/15 s between the alternative illumination, the time lag can be considered small, because the maximum plume velocity is less than 4 mm/s in the present experiment. As optical lens of the stereo camera is placed parallel to the image plane, the present camera configuration is an angular displacement. Although this optical configuration reduces the local distortion of the magnification to some extent compared with that of the Scheimpflug condition, it needs more depth of focus to capture sharp images. Such shortcomings are overcome by higher intensity illumination and larger diameter of tracer particles 40 μm for visualizing the flow. The tracers are nylon sphere particles having a specific gravity of 1.03. They are used for velocity measurements in addition to the liquid-crystal particles, which allow an increase in the accuracy of PIV measurement. The tracer particles are observed about 2 pixels in the image plane, which corresponds to the particle size condition to be analyzed with high accuracy in the PIV measurement (Fujisawa et al., 2004). The liquid crystal particles used in the present measurement is chiral-nematic type, which is encapsulated to a particle of diameter 10 μm. They are mixed with the working fluid of water with a volumetric concentration of 0.3 ppm. The color sensitive temperature range of the liquid crystal is 2 K, which starts at 29 °C. The specific gravity of the particle is 1.02. Note that the frequency response of liquid crystals is an order of msec (Ozawa et al., 1992), which is short enough in comparison with the convective time scale having an order of 100 s.

2.3 Image Analysis for Temperature and Velocity Measurement

The temperature field is evaluated from the color of the liquid crystals suspended in the fluid, while the velocity field is evaluated from stereo PIV measurement in the horizontal plane and from planar PIV measurement in the vertical plane. Once the color images are taken from three 3CCD cameras, images are transformed into HSI color format (Funatani and Fujisawa, 2002). In the temperature analysis, the color to temperature transformation is conducted using the calibrated relationship between the color and the temperature, which is obtained from a uniform temperature field in the test section. Note that the relationship between the HSI color and the temperature is approximated by B-spline curves. Then, the temperature is evaluated by solving the approximated relations of H, S, I with temperatures using a least square method. Note that the non-uniformity of the illumination and the viewing-angle effect of liquid crystals are considered in the measurement using the multi-point calibration technique (Funatani and Fujisawa, 2002). The uncertainty of measurement is 0.08 K at 95 % interval.

Three velocity components in a horizontal plane were measured by stereo PIV. The analysis was carried out using gray-scale images converted from the color images. There is a non-uniform magnification problem at the air-liquid interface, so that three-dimensional calibration technique is introduced in the present analysis (Soloff et al., 1997). The calibration plate used in the present experiment contains 10 × 10 white line rulings having 5 mm interval and 0.5 mm width arranged on a black background. This plate is placed in the test section at 3 different positions in parallel to the light-sheet plane separated by every 3 mm interval to cover the light-sheet thickness. Using these calibration data, the mapping function is determined, which expresses the relationship between the three-dimensional object image and the two-dimensional camera image. It should be noted that the mapping function was approximated by the polynomial expression having a cubic dependence on x

and y, and a quadratic dependence on z.

The PIV analysis between the sequential two images is carried out using the cross-correlation algorithm with a gray level difference method and with the sub-pixel interpolation technique. The interrogation window size is set to 31 × 31 pixels and the candidate region is searched in an area of 45 × 45 pixels to minimize the erroneous velocity vectors, while keeping reasonable spatial resolution. The interrogation window is overlapped by 50 % to obtain the velocity vectors in the whole flow field. Then, the particle displacements from each camera are transformed into three-dimensional velocity vectors in the illumination plane by solving the system of equations for stereo cameras. The velocity uncertainty is 3 % for in-plane velocities and 6 % for out-of-plane velocities at 95 % interval.

2.4 POD Analysis

A snapshot POD method is introduced into the analysis of the experimental data of temperature and velocity field to extract the behavior of coherent structure in the unsteady non-penetrative thermal convection. The basic idea of snapshot POD is that it yields a set of orthogonal eigenfunctions that are optimal in energy representing temporal and spatial correlations of flow variables, such as temperature and velocity. The eigenfunctions of the POD modes of the two-point correlation matrix of temperature and velocity are obtained by solving these equations numerically. The details of the POD analysis using the snapshot method have been described in literature (Sirovich, 1987; Berkooz et al., 1993; Zhou and Hitt, 2004).

3. Results and Discussion

3.1 Visualization of Spoke Structure

The spoke structure near the heated boundary is visualized with the aid of liquid-crystal tracers illuminated by horizontal light sheet. Figure 2 shows an example of spoke structure near the heated boundary (y = 5 mm) after the start of heating 20 minutes at constant heat flux (= 1.9×10^2 W/m^2). Note that the quasi-steady constant growth of mean temperature of the fluid layer is observed within 10 minutes after the start of heating. Therefore, the present experiment is carried out at 20 minutes after the start of heating, where the quasi-steady state of linear growth of temperature with time is observed. For details of quasi-steady state see Keane et al. (1997). In the present experiment, the flux Rayleigh number R_{af} (= α gQ$h^4/\nu^2\kappa$) = 6.5×10^8 (α = thermal expansion coefficient of water, g = gravitational acceleration, Q = mean heat flux, h = height of fluid layer, κ = thermal diffusivity, ν = kinematic viscosity). The image in Fig. 2 corresponds to an area of 70 mm × 100 mm over the heated surface. It can be seen that high temperature lines (blue color) prevail over the heated boundary forming a spoke structure of deformed polygonal shape. The area of green color shows a low temperature area, which is surrounded by high temperature lines of blue color. The spoke structure was visible in a limited period of time about 1 minute in the present experiment, when the fluid temperature passes through the color sensitive temperature range of the liquid crystal. However, the temperature measurement is limited to about the half of the observation time due to the reduced temperature sensitivity of the liquid crystal at the edge of the observation period.

3.2 Instantaneous Contours of Temperature and Velocity Field

The instantaneous contours of temperature and velocity field in the horizontal and vertical planes are measured simultaneously using the liquid-crystal thermometry and stereo velocimetry. Figures 3 and 4 show a few examples of instantaneous temperature and velocity contours in the horizontal and vertical planes, respectively. These results are obtained at every 3 s of time interval. Note that the vertical plane through y = 0 mm is the measurement plane, but it is shown at the end of the image plane not to block the result on the horizontal plane. It can be seen from the temperature contour that the spoke cell on the left-hand side grows in size, and that on the right hand side decreases in size with an increase in elapsed time t. The observation of the vertical image shows that the plumes are generated from the high temperature region of spoke structure, which corresponds to the intersection of bursting lines.

The corresponding velocity field in Fig. 4 shows a similar spoke structure to that observed in the temperature field, but it is vague in some places. This result suggests that the spoke structure is observed along a line of upward velocity in the horizontal plane. It is expected that the upward

velocity is due to the buoyancy force in the high temperature area of the spoke. On the other hand, the upward velocity is observed in the vertical plane where the thermals are found in the temperature contour. Downward velocity occurs in the lower temperature region directing to the

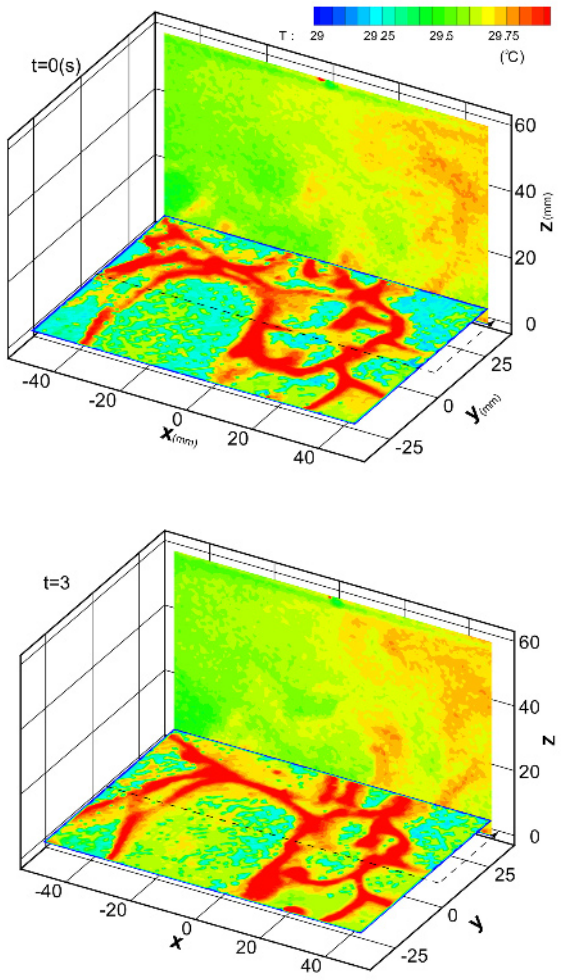

Fig. 3. Three-dimensional expressions of instantaneous temperature field.

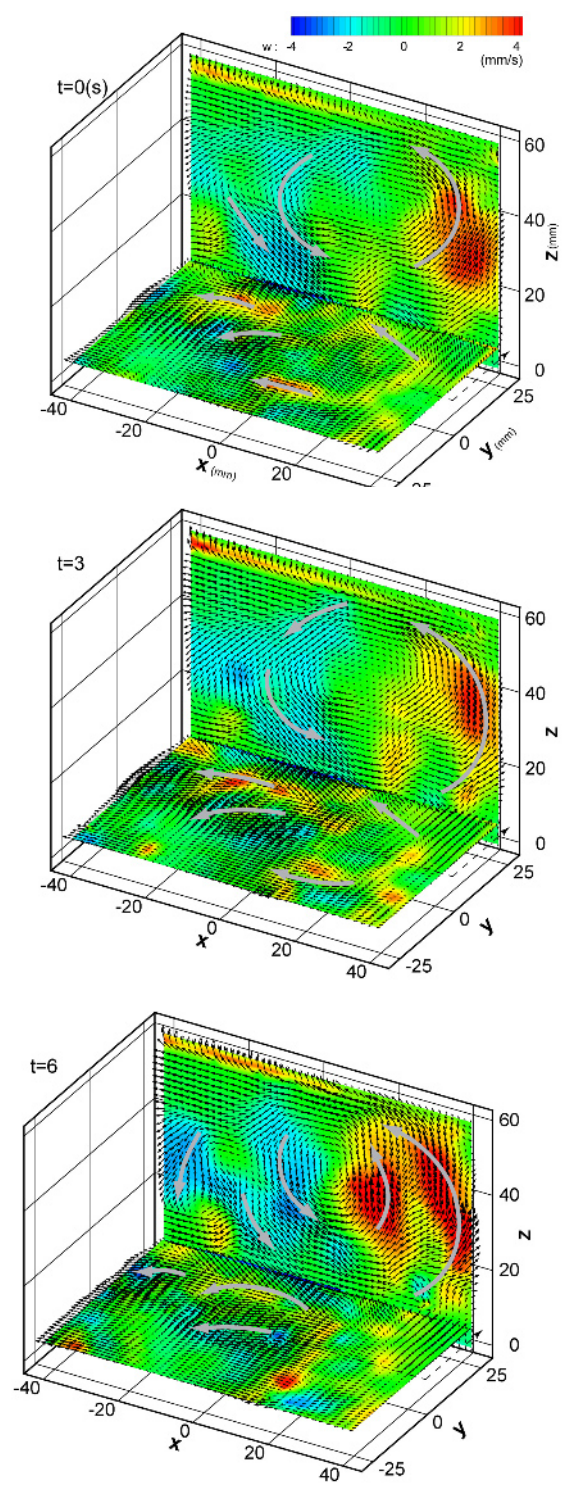

Fig. 4. Three-dimensional expressions of instantaneous velocity field.

center of the spoke structure near the heated boundary and spread in radial direction. It is considered that the upward velocity is generated by the growth of higher temperature region in the spoke structure, which is accelerated in the middle of the fluid layer, and turns back to the lower boundary again due to the fluid motion of lower temperatures. Note that the largest magnitude of velocity fluctuation is observed in the middle of the fluid layer.

3.3 POD Analysis of Temperature and Velocity Field

The snapshot POD method is introduced into the analysis of temperature and velocity field in the present experiment. The analysis is carried out over 200 data sets of temperature and velocity field in the horizontal and vertical planes, which corresponds to a total observation time of 27 s.

Figure 5 shows the distributions of temperature eigenfunctions of the first 3 modes in the horizontal and vertical planes. Note that the magnitude of temperature eigenfunctions in the horizontal plane is larger than those in the vertical plane, so that the different temperature scales are used to express these contours. These results indicate that the positive and negative temperature eigenfunctions are observed alternatively in both horizontal and vertical planes. In the horizontal plane, long streak structure is formed over the heated boundary at the lowest mode n = 1, which corresponds to the bursting lines of the spoke structure, but they do not agree in shape due to the unsteady nature of the spoke. These long streaks are broken into short one with an increase in mode numbers. On the other hand, the temperature eigenfunctions in vertical plane is smaller in magnitude than that observed near the heated boundary, which might be due to the turbulent diffusion of temperature in the middle of the fluid layer. At the lowest mode number n = 1, a large-scale structure corresponding to thermals is observed in the middle of the fluid layer. The positive temperature eigenfunctions correspond to the generation of plume from the lower boundary, and the negative temperature eigenfunctions show relatively lower temperature than the surroundings. With an increase in the mode number, the scale of the structure decreases, but it is still larger than that of the horizontal plane at the same mode numbers, which indicates the growth of the temperature scale in the middle of the fluid layer. The magnitude of temperature eigenfuntions becomes small as the fluid approaches the top boundary.

Figure 6 indicates the distributions of velocity eigenfunctions in the horizontal and vertical planes. The color contour shows the magnitude of vertical velocity eigenfunctions. It is found that the magnitudes of vertical velocity eigenfunctions in the middle of the fluid layer are larger than those near the heated boundary, so that the separate velocity scales are used to express the contours. The velocity eigenfunctions in the horizontal plane indicate the streaky structure, which is also observed in the temperature eigenfunctions over the heated boundary. The velocity eigenfunctions in the vertical plane show the presence of large-scale structure in the velocity field, which is similar to that in the temperature field. The pattern of velocity eigenfunction of n = 1 shows a clockwise vortex in the middle of the fluid layer. With an increase in mode number, the velocity magnitude is reduced and the scale of turbulence is decreased in the fluid layer, which corresponds to the variation of flow pattern with the mode numbers similar to the observation in the temperature eigenfunctions.

4. Conclusions

The temperature and velocity field of unsteady non-penetrative thermal convection is simultaneously measured by the combined liquid-crystal thermometry and stereo velocimetry with high spatial and temporal resolution. The result indicates that the spoke structure is formed near the heated boundary, and the clear convection pattern is created across the fluid layer. It is found that the convection pattern is generated from the high temperature thermals of the spoke structure, which grows across the fluid layer upward, and the low temperature fluid moves down toward the center of the spoke cell and spreads in radial direction along the heated boundary. The POD analysis indicates that the temperature eigenfunctions are larger in magnitude along the spoke structure over the heated boundary, but the velocity eigenfunctions are larger in the middle of the fluid layer. Both results of eigenfunctions show that the spoke structure is formed near the heated boundary and the thermals grow vertically in the middle of the fluid layer. Thus, the POD analysis reproduces main features of thermal convection observed in the instantaneous temperature and velocity field.

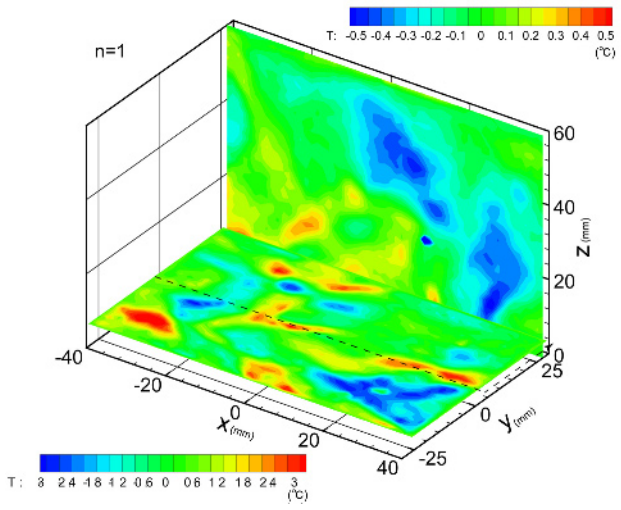

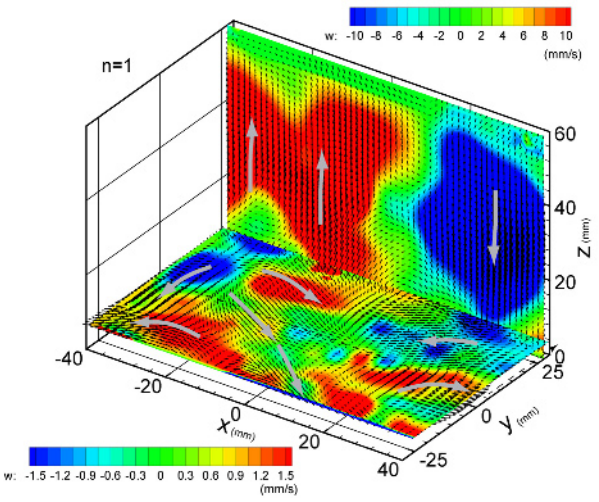

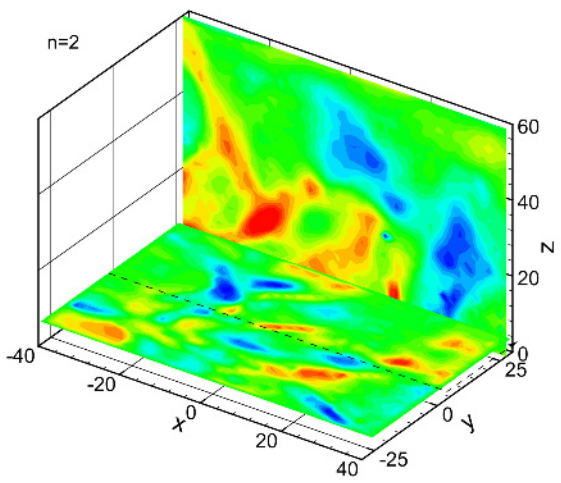

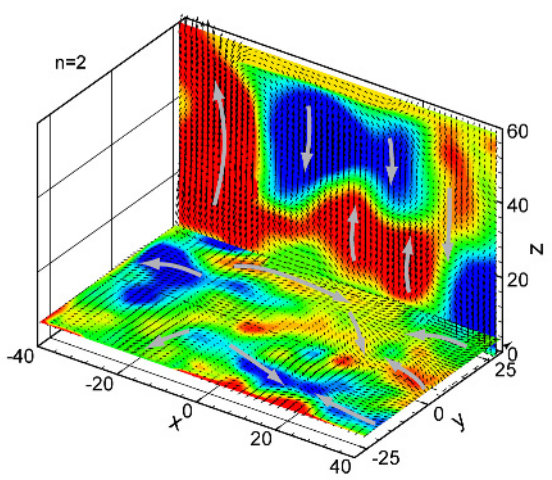

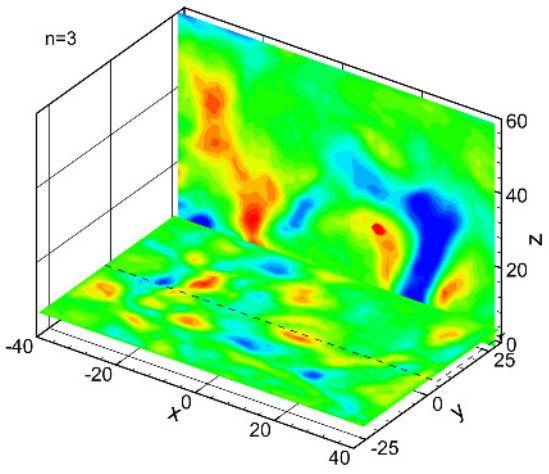

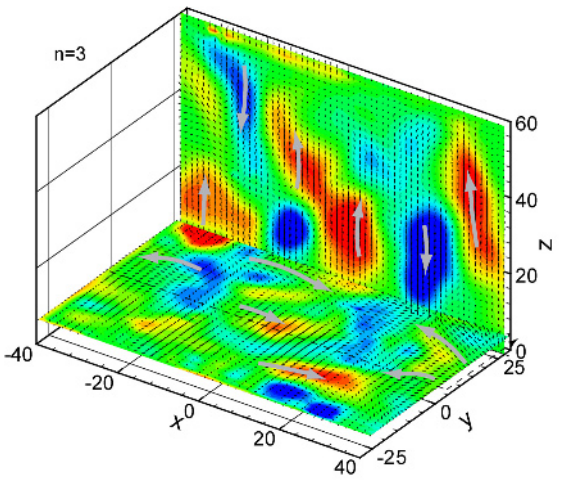

Fig. 5. Three-dimensional expressions of temperature eigenfunctions.

Fig. 6. Three-dimensional expressions of velocity eigenfunctions.

References

Adrian, R. J., Ferreira, R. T. D. S. and Boberg, T., Turbulent Thermal Convection in Wide Horizontal Fluid Layer, Experiments in Fluids, 4 (1986), 121-141.

Balachandar, S., Structure in Turbulent Thermal Convection, Physics of Fluids, A4 (1992), 2715-2726.

Banerjee, J., Bharadwaj, R. and Muralidhar, K., Experimental Study of Convection in a Model Czochralski Crucible Using

Liquid Crystal Thermography, Journal of Visualization, 9-1 (2006), 111-120.
Berkooz, G., Holmes, P. and Lumley, J. L., The Proper Orthogonal Decomposition in the Analysis of Turbulent Flows, Annual Review of Fluid Mechanics, 25 (1993), 539-575.
Castaing, B., Gunaratine, G., Heslot, F., Kadanoff, L., Libchaber, A., Thomas, S., Wu, X. Z., Zaleski, S. and Zannetti, G., Scaling of Hard Thermal Turbulence in Rayleigh-Bérnard Convection, Journal of Fluid Mechanics, 204 (1989), 1-30.
Dabiri, D. and Gharib, M., The Effects of Forced Boundary Conditions on Flow within a Cubic Cavity Using Digital Particle Image Thermometry and Velocimetry (DPITV), Experimental Thermal and Fluid Science, 13 (1996), 349-363.
Fujisawa, N. and Adrian, R. J., Three-dimensional Temperature Measurement in Turbulent Thermal Convection by Extended Range Scanning Liquid Crystal Thermometry, Journal of Visualization, 1-4 (1999), 355-364.
Fujisawa, N., Funatani, S. and Katoh, N., Scanning Liquid-crystal Thermometry and Stereo Velocimetry for Simultaneous Three-dimensional Measurement of Temperature and Velocity Field in a Turbulent Rayleigh-Bernard Convection, Experiments in Fluids, 38 (2005), 291-303.
Fujisawa, N., Nakajima, T., Katoh, N. and Hashizume, Y., An Uncertainty Analysis of Temperature and Velocity Measured by Stereo Liquid-crystal Thermometry and Velocimetry, Measurement Science and Technology, 15 (2004), 799-806.
Funatani, S. and Fujisawa, N., Simultaneous Measurement of Temperature and Three Velocity Components in Planar Cross-section by Liquid Crystal Thermometry Combined with Stereoscopic Particle Image Velocimetry, Measurement Science and Technology, 13 (2002), 1197-1205.
Gluckman, B. J., Willaime, H. and Gollub, J. P., Geometry of Isothermal and Isoconcentration Surfaces in Thermal Turbulence, Physics of Fluids, A5 (1993), 647-661.
Inagaki, T., Hatori, M., Suzuki, T. and Shiina, Y., Heat Transfer and Fluid Flow of Benard-Cell Convection in Rectangular Container with Free Surface Sensed by Infrared Thermography, Journal of Visualization, 9-2 (2006), 145-160.
Keane, R. D., Fujisawa, N. and Adrian, R. J., Unsteady Non-penetrative Thermal Convection from Non-uniform Surfaces, TAM Report, UILU-ENG-97-6008 (1997).
Ozawa, M., Müller, U., Kimura, I. and Takamori, T., Flow and Temperature Measurement of Natural Convection in a Hele-Shaw Cell Using a Thermo-sensitive Liquid-crystal Tracer, Experiments in Fluids, 12 (1992), 213-222.
Prasad, A. K. and Gonunguntla, P. V., Turbulence Measurements in Nonpenetrative Thermal Convection, Physics of Fluids, 8 (1996), 2460-2470.
Schmidt, H. and Schumann, U., Coherent Structure of the Convective Boundary Layer Derived from Large-eddy Simulations, Journal of Fluid Mechanics, 200 (1989), 511-562.
Sirovich, L., Turbulence and the Dynamics of Coherent Structures, Quartarly Applied Mathematics, XLV(1987), 561-590.
Soloff, S. M., Adrian, R. J. and Liu, Z. C., Distortion Compensation for Generalized Stereoscopic Particle Image Velocimetry, Measurement Science and Technology, 8 (1997), 1441-1454.
Sparrow, E. M., Husar, R. B. and Goldstein, R. J., Observation and Other Characteristics of Thermals, Journal of Fluid Mechanics, 41 (1970), 793-800.
Tamai, N. and Asaeda, T., Sheetlike Plumes near a Heated Bottom Plate at Large Rayleigh Number, Journal of Geophysical Research, 89 (1984), 727-734.
Willis, G. E. and Deardorff, J. W., Laboratory Observation of Turbulent Penetrative-convection Planforms, Journal of Geophysical Research, 20 (1979), 295-302.
Zhou, X. and Hitt, D. L., Proper Orthogonal Decomposition Analysis of Coherent Structures in a Transient Buoyant Jet, Journal of Turbulence, 5 (2004), 1-21.

Author Profile

Nobuyuki Fujisawa: After graduating from Tohoku University (Dr E. 1983), he joined Gunma University and worked as an associate professor since 1991. He has been a professor of Niigata University since 1997, and currently a President of Visualization Research Center at Niigata University. His current research interests are flow visualization, non-intrusive measurement of temperature and velocity in thermal flow and combusting flow, and mass transport phenomena of flow accelerated corrosion problems.

Masataka Watanabe: He received his M.Sc.(Eng.) in Mechanical Engineering in 2007 from Niigata University. Now, he works for FA and CNC, FANUC in Yamanashi prefecture, Japan.

Yuji Hashizume: He received M.Sc.(Eng.) in Mechanical Engineering in 2002 from Niigata University and Ph.D. in 2005 from Shinshu University. He worked at Graduate School of Niigata University as a postdoctoral fellow. Currently, he works in KGT Inc. His research interests are experimental flow visualization, image processing, image measurement for application to thermal flow phenomenon.